intersystem crossing (W. M. Nau, W. Adam, J. C. Scaiano, *J. Am. Chem. Soc.* **1996**, *118*, 2742 – 2743).
[20] C. Reichardt, *Solvents and Solvent Effects in Organic Chemistry*, VCH, Weinheim, **1988**.
[21] Protic solvents caused again an *increase* in the rate constants, for example, the rate constants in aqueous solution were virtually the same as in cyclohexane. This effect can be due to specific solvation (hydrogen bonding) and the larger singlet-excitation energy of n,π*-excited states in protic solvents, cf. $\lambda_{max}$ of DBO in hexane (378 nm) versus water (364 nm).
[22] T. R. Evans, *J. Am. Chem. Soc.* **1971**, *93*, 2081 – 2082.
[23] P. S. Engel, A. Kitamura, D. E. Keys, *J. Org. Chem.* **1987**, *52*, 5015 – 5021.
[24] W. Adam, A. Nikolaus, *Eur. J. Org. Chem.* **1998**, 2177 – 2179.
[25] For the quantitative prediction of the free enthalpy of electron transfer[1] we used $E_{ox}(NEt_3) = 0.96$ V (vs. saturated calomel electrode (SCE)),[33] $E_{p,red}(DBO) = -2.8$ V (vs. SCE in acetonitrile/hanging mercury drop electrode (HMDE), this work), $E^*(^1DBO^*) = 3.30$ eV,[19] $E_{red}(Ph_2CO) = -1.83$ V (vs. SCE in acetonitrile),[28] $E^*(^3Ph_2CO^*) = 3.00$ eV,[28] taking the Coulomb term as $-0.06$ eV in acetonitrile.
[26] K. Kikuchi, Y. Takahashi, T. Katagiri, T. Niwa, M. Hoshi, T. Miyashi, *Chem. Phys. Lett.* **1991**, *180*, 403 – 408.
[27] X. Allonas, Ecole Nationale Supérieure de Chimie de Mulhouse, unpublished results.
[28] P. J. Wagner, R. J. Truman, A. E. Puchalski, R. Wake, *J. Am. Chem. Soc.* **1986**, *108*, 7727 – 7738.
[29] J. Gersdorf, J. Mattay, H. Görner, *J. Am. Chem. Soc.* **1987**, *109*, 1203 – 1209.
[30] P. Jacques, *J. Photochem. Photobiol. A* **1991**, *56*, 159 – 163.
[31] I. R. Gould, R. H. Young, L. J. Mueller, S. Farid, *J. Am. Chem. Soc.* **1994**, *116*, 8176 – 8187.
[32] P. Jacques, X. Allonas, M. von Raumer, P. Suppan, E. Haselbach, *J. Photochem. Photobiol. A* **1997**, *111*, 41 – 45.
[33] W. Adam, J. N. Moorthy, W. M. Nau, J. C. Scaiano, *J. Am. Chem. Soc.* **1997**, *119*, 6749 – 6756.
[34] T. M. Bockman, S. M. Hubig, J. K. Kochi, *J. Am. Chem. Soc.* **1998**, *120*, 2826 – 2830.
[35] Y. P. Tsentalovich, H. Fischer, *J. Chem. Soc. Perkin Trans. 2* **1994**, 729 – 733.
[36] M. Hild, H.-D. Brauer, *Ber. Bunsen-Ges. Phys. Chem.* **1996**, *100*, 1210 – 1216.
[37] Emission from singlet exciplexes involving n,π*-excited states has never been observed to our knowledge.
[38] E. Lippert, *Z. Naturforsch. A* **1955**, *10*, 541 – 545.
[39] N. Mataga, Y. Kaifu, M. Koizumi, *Bull. Chem. Soc. Jpn.* **1956**, *29*, 465 – 471.
[40] J. J. P. Stewart, *J. Comput. Chem.* **1989**, *10*, 209 – 220.
[41] U. Maharaj, I. G. Czizmadia, M. A. Winnik, *J. Am. Chem. Soc.* **1977**, *99*, 946 – 948.
[42] M. G. Ivanov, E. Z. Zhuravlev, Y. Dergunov, T. P. Elizarova, *Zh. Obshch. Khim.* **1990**, *60*, 1209 – 1212.
[43] M. D. Harmony, T. L. Talkinkton, R. N. Nandi, *J. Mol. Struct.* **1984**, *125*, 125 – 130.
[44] H. Shimamori, H. Uegaito, K. Houdo, *J. Phys. Chem.* **1991**, *95*, 7664 – 7667.
[45] M. Terazima, K. Okamoto, N. Hirota, *J. Phys. Chem.* **1993**, *97*, 13387 – 13393.
[46] For diisopropylsulfide the UHF-PM3 calculation gave $\mu_B = 2.1$ D and for the corresponding exciplex $\mu_{AB} = 4.0$ D.
[47] In an effort to observe a "normal" solvent effect we examined also triphenylamine, which is a better donor than triethylamine (Table 2). However, the solvent effect for this better amine donor was very similar as for triethylamine. Although this result may be in part related to the increase in molecular size of triphenylamine, which would tend to balance the donor strength effect in Equation (1), a *C* value could not be estimated. The UHF-PM3 calculation does not produce minimum exciplex structures in the case of aromatic amines, which differ from aliphatic amines in that they act as "π" rather than "n" donors (cf. P. Jacques, X. Allonas, *Chem. Phys. Lett.* **1995**, *233*, 533 – 537).

# An Inorganic Tire-Tread Lattice: Hydrothermal Synthesis of the Layered Vanadate $[N(CH_3)_4]_5V_{18}O_{46}$ with a Supercell Structure**

Bryan E. Koene, Nicholas J. Taylor, and Linda F. Nazar*

There has been much recent interest in preparing new vanadium oxides owing to their promise as anodes in secondary lithium batteries and electrochromic devices.[1–3] The catalytic properties of vanadium oxides also make these materials viable candidates as heterogeneous catalysts. An inviting synthetic route that deviates from traditional solid-state high-temperature synthesis is hydrothermal chemistry at relatively low temperatures (120 – 250 °C) and pressures with organic cations as templating agents. Recent developments in this field have proven that it is a viable method for the preparation of many novel two-dimensional materials, especially vanadium oxides. To date, only five truly unique host inorganic lattices have been synthesized, although each lattice can be formed with one of several organic cations in most cases. The lattices, indicated by square brackets, include $[V_4O_{10}]^-$ in the presence of tetramethylammonium (TMA) ions;[4] $[V_4O_{10}]^{2-}$ in the presence of ethylenedamine (en), piperazine (pip),[5] or diaminopropane;[6] and $[V_6O_{14}]^{2-}$ in the presence of 1,4-Diazabicyclo[2.2.2]octan (dabco).[7] Other frameworks that are very closely related to $[V_6O_{14}]^{2-}$ were also recently reported, namely, $(TMA)_2[V_6O_{14}]$[8] and $[Zn(en)_2]^{2+}[V_6O_{14}]$.[9] The mechanism by which these inorganic and organic components assemble under hydrothermal conditions is currently the subject of intense research but is not yet understood. Cooperative organization of organic and inorganic phases has been alluded to in some cases. The organic cation also acts as a reducing agent in the synthesis of transition metal oxides, and this complicates the dissolution and nucleation processes.

We report here the highly unusual layered vanadate $(TMA)_5V_{18}O_{46}$, whose structure is sufficiently distinct from of those other metal oxides that it has no precedent in the literature. The lattice is self-assembled from two distinct $[V_9O_{23}]$ building blocks, neither of which is known to form repeating lattices on its own, to form a supercell arrangement. One building block is neutral, and the other carries localized electrons and is negatively charged. The organic cations reside between the layers. Formation of this unusual lattice arrangement appears to be driven by thermodynamic factors that minimize strain in the "mixed" alternating lattice.

$(TMA)_5V_{18}O_{46}$ was prepared by mixing $V_2O_5$ (182 mg, 1.0 mmol), $V_2O_3$ (50 mg, 0.33 mmol), $[N(CH_3)_4]Cl$ (110 mg,

[*] Prof. L. F. Nazar, B. E. Koene, N. J. Taylor
Department of Chemistry
University of Waterloo
Waterloo, ON, N2L 3G1 (Canada)
Fax: (+1) 519-746-0435
E-mail: lfnazar@uwaterloo.ca

[**] This work was supported by the NSERC (Canada) through the operating and strategic research programs. G. R. Goward and J. Britten are thanked for confirming the structure with an independent determination.

  1433-7851/99/3819-2888 $ 17.50+.50/0 

1.0 mmol), and $[N(CH_3)_4]OH$ (5.0 mmol), and then adjusting the pH to 5.0 by the dropwise addition of $HNO_3$. The mixture was heated under autogeneous pressure in an Teflon-lined autoclave at 170 °C for 2 d. The resulting product was a mixture of black crystalline phases, of which approximately 10 % was the title compound. The characteristic long, hexagonally distorted morphology of the crystals allowed them to be readily separated from the other phases. Another layered vanadate ($(TMA)V_4O_{10}$) was recovered from this reaction mixture (40 %), along with the well-known polyoxovanadate cluster $(TMA)_6V_{15}O_{36}\cdot Cl\cdot 4H_2O$ (40 %), and a fourth, unknown phase (10 %). These black, octagonal crystals have a very long unit cell length along one axis (69.5 Å) and a high degree of disorder perpendicular to the layers. They appear to be a larger disordered supercell of the title compound, although further details await structural refinement.

The asymmetric unit cell of $(TMA)_5V_{18}O_{46}$ is shown in Figure 1a without the TMA cations. Several unusual structural characteristics indicate that the structure is intermediate between two different phases. First, the 18 unique vanadium atoms are arrayed in a "block" motif in the layers, in contrast to regular ordering of polyhedra in the lattice in all other structurally characterized metal oxides prepared by solid-state routes or hydrothermal synthesis. The lattice is best considered as consisting of two periodic "intergrowth" segments that have similarities to other known vanadates. The two segments that form strips within the layers are shown more clearly in a polyhedral motif perpendicular to the layers (Figure 1b). The building blocks are compared to other known phases in Figure 2, in which a portion of the $(TMA)_5V_{18}O_{46}$ structure (Figure 2b) is shown along three orthogonal directions together with the unit cells of $\alpha$-$V_2O_5$ and $(TMA)V_4O_{10}$. The section of the lattice between V3 and V10 (Block A) resembles $\alpha$-$V_2O_5$, although the square pyramids share corners with chains of polyhedra disposed in an opposite orientation, unlike $\alpha$-$V_2O_5$, in which the corresponding corner-sharing square pyramids have the same orientation (Figure 2a). This topology is, however, similar to the network of $V_{2-x}Mo_xO_5$ if the sites in the latter are regarded as square-pyramidal.[10] The resultant block is slightly curved, viewed

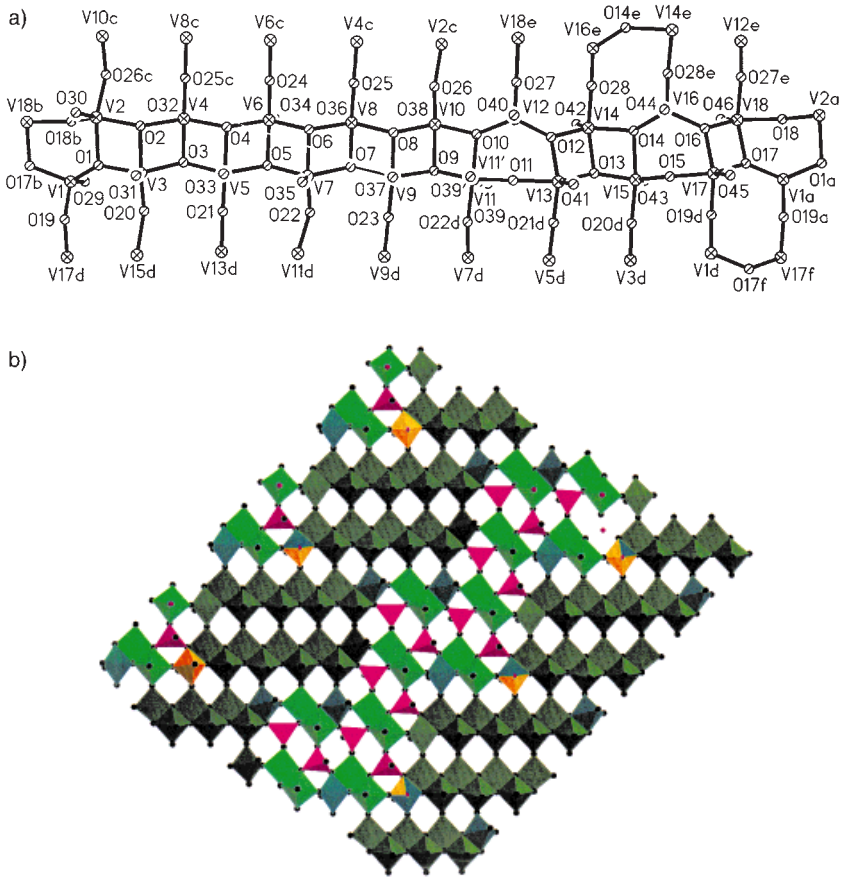


Figure 1. a) Asymmetric unit cell of $[N(CH_3)_4]_5V_{18}O_{46}$. In the disorder about V11/V11′, the square pyramid is flipped by 180° for about ¼ of its occurrence in the lattice; four inversion centers exist on positions occupied by O25, O27 and adjacent to O14, O17. Symmetry codes: a: $1+x$, $1+y$, $1+z$; b: $-1+x$, $-1+y$, $-1+z$; c: $1-x$, $1+y$, $1+z$; d: $1-x$, $1-y$, $1-z$; e: $2-x$, $1-y$, $2-z$. b) View of $[N(CH_3)_4]_5V_{18}O_{46}$ in polyhedral motif, perpendicular to the layers.

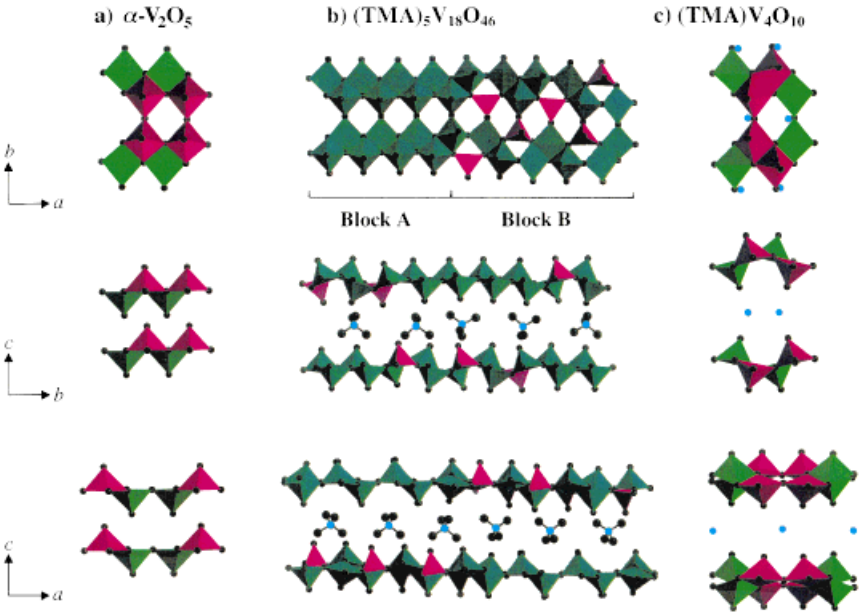


Figure 2. Polyhedral depiction of the structure of $[N(CH_3)_4]_{10}V_{36}O_{92}$ along the three different crystal axes, shown with respect to the labeling adopted for the $V_2O_5$ axes, in comparison with other vanadium oxides; a) $\alpha$-$V_2O_5$; b) $(TMA)_5V_{18}O_{46}$; c) $(TMA)V_4O_{10}$.

  1433-7851/99/3819-2889 $ 17.50+.50/0 

parallel to the layers, whereas the corresponding view of the $\alpha$-$V_2O_5$ layers shows they are completely flat.

The second block, between V11 and V1a (Block B), is more irregular. The three tetrahedra at V1, V12, and V15 can be considered to be very highly distorted square pyramids with very long equatorial bonds to oxygen atoms 018, 011, and 015, respectively ($\approx$2.8 Å). If the square pyramids were regular (i.e., if the equatorial bonds were all of the same length), this block would effectively have the same topology as (TMA)-$V_4O_{10}$ (Figure 2c). Alternatively, if these sites are classified as tetrahedral, this block can be considered to be a disordered combination of the framework structures of $(H_2dabco)V_6O_{14}^{7-}$ and $(H_2pip)V_4O_{10}^{5-}$, since the pairs of square pyramids with an *anti* disposition alternate with those of *syn* disposition along the chain direction. A common characteristic of Block B and the related polyhedral networks is edge-sharing square pyramids disposed in the same direction, an arrangement which is exclusively found in layered vanadates prepared by hydrothermal methods, as opposed to high-temperature solid-state reactions. Hydrothermal synthesis does not always result in such an organization, however, as the alkyldiammonium $[V_4O_{10}]^{2-}$ vanadates[5] have edge-sharing $VO_5$ square pyramids alternatingly oriented in different directions.

The similarly oriented adjacent square pyramids in Block B are tilted substantially away from one another to give highly puckered layers due to the repulsion of the adjacent axial oxygen atoms. Hence, the layers of $(TMA)_{45}V_{18}O_{46}$ are slightly curved in Block A, in which the layers are similar to $\alpha$-$V_2O_5$ (V3 – V1), but are puckered in Block B, as in $(TMA)V_4O_{10}$, in which repulsion between axial oxygen atoms is observed (V11 – V18). The ultimate result of such repulsion effects are polyoxovanadium clusters, in which similarly oriented square pyrimids are exclusively observed (i.e., all axial oxygen atoms point outwards, and the central vanadium cation in the square pyramidal base interacts with an anion at the center of the cluster). Müller et al.[11] showed that the repulsive interaction between the terminal oxygen atoms directly influences the curvature of the shell. In a similar way, the corrugated layers we observe may be influenced by such interactions. Hence, the subtle, but distinct, curvature of Block A may represent an intermediate step en route to cluster formation.

The average oxidation state of vanadium in the title compound of $V^{4.83+}$ is manifested in an unusual distribution of $V^{4+}$ in the structure. The relative localization of the negative charge over the 15 square-pyramidal sites in the unit cell of the latter can be calculated from valence bond sums (Table 1). The partially reduced vanadium ions ($V^{<5+}$) are localized as weakly interacting dimer pairs on V13/V14 and V17/V18, giving rise to average oxidation states of 4.1/4.3 and 4.5/4.7, respectively, from valence sum calculations. These are highlighted in the view along the direction perpendicular to the layers (Figure 1b). The structural distortion is apparently driven by pinching of the structure at the dimer "defects". This also results in an alternating three-dimensional tire-tread pattern of the strips along the direction perpendicular to the layers (Figure 3). Thus, the neutral strips containing "$V_2O_5$"-type blocks are interleaved with the structurally distorted strips containing negatively charged blocks with localized reduced vanadium centers. This gives rise to the superlattice structure of Block A/Block B moities about 12 Å in width. This probably arises to relieve the structural strain that would arise from either lattice alone. Note that neither building block alone is known to form a repeating lattice.

Table 1. Valency of vanadium in $[(CH_3)_4N]_5V_{18}O_{46}$(1) from valence bond sum calculations.

| V atom | Valency | V atom | Valency |
|---|---|---|---|
| V1 – V11 | 5.00 ± 0.1 | | |
| V13 | 4.40 | V16 | 4.92 |
| V14 | 4.09 | V17 | 4.48 |
| V15 | 4.98 | V18 | 4.23 |

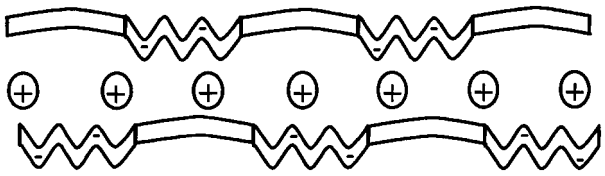

Figure 3. Schematic representation of $[N(CH_3)_4]_5V_{18}O_{46}$ illustrating the structure in a direction parallel to the layers; the slightly curved portions represent Block A, and the puckered portions with the localized negative charges Block B.

While crystallization of this unique framework is apparently driven by the relief of lattice strain, its assembly is presumably controlled by kinetic factors. Furthermore, the presence of preformed "building blocks" in solution at some stage in the nucleation process is implicated by the structure. Block A, for example, may arise from preferential dissolution of $\alpha$-$V_2O_5$ along the direction of the corner-joined ribbons. The reverse of this process, "oxolation",[12] is thought to take part in the growth of xerogel $V_2O_5$ from vanadate solutions. The structure of Block B is related to that of $(TMA)V_4O_{10}$ (vide supra), which also crystallized from the mother liquor. Note that the oxidation state of vanadium in the latter compound is +4.75, whereas the average oxidation state in the $[V_9O_{23}]^{5-}$ units that constitute Block B is lower (+4.55). In addition, although the release of the species, the pH value, and the temperature undoubtedly play a part in the rate of nucleation and crystal growth, redox chemistry is also a factor. Here, as in all hydrothermally prepared transition metal oxides, crystallization is partly controlled by the rate of reduction of the $V_2O_5$ in the synthesis liquor, which usually occurs by reaction with the organic compound in solution (TMA). In this case, the presence of $V_2O_3$ provides another source. We propose that partial reduction of the vanadium centers by reaction with $V_2O_3$ during incipient nucleation of the $[V_4O_{10}]$-like lattice building blocks may give rise to Block B units, which then crystallize to form a repeating lattice by self-assembly with Block A.

*Experimental Section*

Crystal data for $[N(CH_3)_4]_5V_{18}O_{46}$: A crystal of dimensions 0.036{101} × 0.14{001} × 0.18{101} × 0.36{111} × 0.125{013} mm was selected for data

  1433-7851/99/3819-2890 $ 17.50+.50/0 

collection on a Siemens P4 automated diffractometer ($Mo_{K\alpha}$, $\lambda = 0.71073$ Å, $T = 295$ K); space group $P\bar{1}$; $a = 12.660(3)$, $b = 15.359(3)$, $c = 16.963(3)$ Å, $\alpha = 78.72(3)$, $\beta = 74.37(3)$, $\gamma = 83.33(3)^\circ$, $V = 3108.0(11)$ Å$^3$, $Z = 2$, $\rho_{calcd} = 2.145$ g cm$^{-3}$. Cell parameters from 25 reflections ($20 < 2\theta < 28^\circ$), 8459 reflections collected by $\omega$-scan method ($\Delta\omega = 1.2^\circ$): $4 < 2\theta < 46^\circ$, $0 \le h \le 13$, $-16 \le k \le 16$, $-17 \le l \le 18$; 4627 reflections observed [$F \ge 4\sigma(F)$]. After data reduction (Lorentzian and polarization corrections; absorption correction by face-indexed analytical method; min./max. equivalent transmission factors: 0.6994, 0.9129) and merging ($R_{int} = 0.0235$), the structure was solved by direct methods with SHELXTL PLUS, and refined by full-matrix least-squares methods. Anisotropic thermal factors were refined for V and O atoms only. $\Delta\rho = -0.59$, $+1.11$ e Å$^{-3}$ associated with disorder on V11/V11′ (see legend to Figure 1). Final residuals: $R(F) = 0.0487$, $wR_2(F) = 0.0492$. Further details on the crystal structure investigation may be obtained from the Fachinformationszentrum Karlsruhe, D-76344 Eggenstein-Leopoldshafen, Germany (fax: (+49) 7247-808-666; e-mail: crysdata@fiz-karlsruhe.de), on quoting the depository number CSD-410088.

Received: August 28, 1998
Revised version: June 10, 1999 [Z12349IE]
German version: *Angew. Chem.* **1999**, *111*, 3065 – 3068

**Keywords:** hydrothermal synthesis · polyoxometalates · template synthesis · vanadium

[1] C. R. Walk in *Lithium Batteries* (Ed.: J. P. Gabano), Academic Press, New York, **1983.**
[2] F. Garcia-Alvarado, J. M. Tarascon, B. Wilkens, *J. Electrochem. Soc.* **1992**, *139*, 3206.
[3] W. Li, J. R. Dahn, D. S. Wainwright, *Science* **1994**, *264*, 1115.
[4] a) E. A. Boylan, T. Chirayil, J. Hinz, P. Zavalij, M. S. Whittingham, *Solid State Ionics* **1995**, *90*, 1; b) P. Zavalij, M. S. Whittingham, E. A. Boylan, V. K. Pecharsky, R. A. Jacobson, *Z. Kristallogr.* **1996**, *211*, 464.
[5] a) D. Riou, G. Férey, *Inorg. Chem.* **1995**, *34*, 6520; b) D. Riou, G. Férey, *J. Solid State Chem.* **1995**, *120*, 137.
[6] a) D. Riou, G. Férey, *J. Solid State Chem.* **1995**, *120*, 137; b) Y. Zhang, C. J. O'Conner, A. Clearfield, R. C. Haushalter, *Chem. Mater.* **1996**, *8*, 595; c) Y. Zhang, R. C. Haushalter, A. Clearfield, *Inorg. Chem.* **1996**, *35*, 4950.
[7] L. F. Nazar, B. E. Koene, J. F. Britten, *Chem. Mater.* **1996**, *8*, 327.
[8] T. G. Chirayil, E. A. Boylan, M. Mamak, P. Y. Zavalij, M. S. Whittingham, *Chem. Commun*. **1997**, 33.
[9] Y. Zhang, F. R. DeBord, C. J. O'Connor, R. C. Haushalter, A. Clearfield, J. Zubieta, *Angew. Chem.* **1996**, *108*, 1067; *Angew. Chem. Int. Ed. Engl.* **1996**, *35*, 989.
[10] L. Kihlborg, *Acta Chem. Scand.* **1967**, *21*, 2495.
[11] A. Müller, R. Rohlfing, E. Krickemeyer, H. Bögge, *Angew. Chem.* **1993**, *105*, 916; *Angew. Chem. Int. Ed. Engl.* **1993**, *32*, 909.
[12] J. Livage, *Proceedings of the 1st International Conference on Composites: Design for Performance* (Lake Louise, Canada) **1977**, 45 – 52.

## Combinatorial Methods for the Synthesis of Aluminophosphate Molecular Sieves**

Kwangwook Choi, David Gardner, Nicole Hilbrandt, and Thomas Bein*

The optimization of existing hydrothermal procedures for the synthesis of microporous materials and the discovery of new phases depends on effective processing and structural screening methodologies. In view of the tremendous impact of combinatorial techniques in the areas of organic,[1] biochemical,[2] and inorganic[3] chemistry, it appears attractive to develop a combinatorial approach for the hydrothermal synthesis of microporous materials. Akporiaye and co-workers demonstrated the application of combinatorial methods for the hydrothermal synthesis of zeolites with a multiple autoclave;[4] the recovery and identification of the obtained phases required individual sample manipulation. Recently, Maier and co-workers reported the microgram-scale hydrothermal synthesis of microporous materials in an array format on a Si wafer which allowed for automated X-ray diffractometry.[5]

We have developed a new methodology based on automatic dispensing of reagents into autoclave blocks, followed by synthesis, isolation, and automated structure analysis without any manipulation of individual samples. Our reaction chambers ("multiclaves") are Teflon blocks (36 mm diameter, with 8 holes (6 mm diameter) or 19 holes (4.5 mm diameter), 25 mm in hole depth) that provide an inert reaction environment. This allows us to use reactant volumes of 150 – 300 μL per hole. A thin sheet and a lid of Teflon covers the reaction vessel, which is then sealed inside a specially designed stainless steel autoclave. The reagents are dosed directly into the multiclaves using a commercially available pipette robot, or a custom-built robot[6] which can inject multiple liquid reagents. After hydrothermal synthesis, the washing of the sample array by filtration and preparation of libraries is done with a custom-designed centrifuge apparatus,[7] which allows almost quantitative product recovery. The resulting products are identified in transmission using either a standard X-ray powder diffractometer or a rotating anode diffractometer with CCD detector. In both cases, an automated xy stage is used for sample translation. The advantages of our methodology include reduced reagent consumption by direct dosing at the microliter scale, production of multi-milligram sample

[*] Prof. T. Bein,[+] K. Choi, D. Gardner, Dr. N. Hilbrandt
Department of Chemistry
Purdue University
West Lafayette, IN 47906 (USA)
Fax: (+1) 765-494-0239
E-mail: tbein@chem.purdue.edu

[+] New address:
Institut für Organische Chemie der Universität München (LMU)
Butenandtstrasse 5 – 13(E)
D-81377 München (Germany)
Fax: (+49) 89-2180-7624
E-mail: tbein@cup.uni-muenchen.de

[**] Funding from the US National Science Foundation, the Purdue Research Foundation (K.C.), and the Humboldt Foundation (N.H.) is greatly appreciated. We thank Dr. P. Fanwick for his support during the X-ray data collection.

  1433-7851/99/3819-2891 $ 17.50+.50/0 